JOURNAL OF APPLIED ELECTROCHEMISTRY 23 (1993) 113–119

Effect of gas evolution on dispersion in an electrochemical reactor

W. S. WU, G. P. RANGAIAH

Department of Chemical Engineering, National University of Singapore, Singapore 0511, Republic of Singapore

M. FLEISCHMANN

Department of Chemistry, The University, Southampton SO9 5NH, Great Britain

Received 6 May 1992; revised 7 July 1992

Gas evolution at electrodes is encountered in many electrochemical processes, and the resulting gas bubbles affect mixing or dispersion in the neighbouring liquid. Experiments were conducted to study the effect of electrogenerated gas bubbles on dispersion in the fluid close to wall in a parallel-plate electrochemical reactor. Platinum microelectrodes and copper electrodes were used to generate gas (hydrogen or oxygen depending on polarity) bubbles and to measure dispersion, respectively. Estimated void fraction of gas bubbles was less than 0.01. Response curves were modelled using the axially dispersed plug flow model. Results obtained indicate that mean residence time of marked material (i.e. fluid close to wall) is almost unaffected by gas bubbles. Dispersion coefficient, however, increases with gas evolution at low liquid flow rates (say, for Reynolds number less than 100); but it is unaffected at higher flow rates. The effect of hydrogen and oxygen bubbles on dispersion under the range of conditions studied, appears to be similar.

List of symbols

C normalized concentration ($mol\,cm^{-3}\,s^{-1}$)
d average break off diameter of gas bubble (cm)
$\bar{D}$ dispersion coefficient ($cm^2\,s^{-1}$)
d_h hydraulic diameter (cm)
g acceleration due to gravity ($cm\,s^{-2}$)
L distance between marker and detector electrodes (cm)
Pe Peclet number = $\bar{u}L\bar{D}^{-1}$ (dimensionless)
Re Reynolds number = $Ud_h\nu_L^{-1}$ (dimensionless)
s cell or inter-electrode gap (cm)
t time (s)
U mean bulk velocity ($cm\,s^{-1}$)
$\bar{u}$ average velocity of marked material ($cm\,s^{-1}$)
u_b bubble rise velocity in a swarm ($cm\,s^{-1}$)
u superficial velocity ($cm\,s^{-1}$)
u_0 rise velocity of a single bubble in a quiescent liquid ($cm\,s^{-1}$)
y thickness of marked layer (cm)

Greek symbols

θ dimensionless time = $t\tau^{-1}$
τ residence time of marked material (s)
ν kinematic viscosity ($cm^2\,s^{-1}$)
ρ density ($g\,cm^{-3}$)
ε void fraction (volumetric gas flow/gas and liquid flow)

Subscripts

L liquid phase
G gas phase

1. Introduction

In many electrochemical processes, gas is evolved at the cathode, anode or both electrodes. As all electrochemical reactions take place at the electrode–solution interface, the formation, growth and detachment of electrogenerated bubbles have a profound effect on the overall process. In the production of chlorine and water electrolysis, attempts are being continually made to reduce the overvoltage and the nonuniform current distribution caused by the presence of bubbles. In metal-winning cells, air is sparged to enhance the rate of mass transfer at the electrode. Many electro-organic syntheses involve co-evolution of gas, which leads to a change in the micro-environment due to the mixing caused by bubbles. This mixing affects the distribution of space–time histories of reactants and intermediates, and thus influences the selectivity and yield of the process [1].

The presence of gas in an electrochemical reactor affects: (i) the ohmic resistance of cells and, hence, the power consumption, (ii) the mixing history in the reactor (both in the bulk flow and in the phase close to electrodes) and (iii) the mass transfer to and from electrodes. There have been extensive investigations of the ohmic resistance of cells [1–5] and of mass transfer to/from electrodes [6–8]. But measurements of the effect of bubbles on the mixing history have been confined to the influence of gas sparging on the core flow of a parallel plate channel reactor [9].

In the absence of gas, mixing or dispersion and the flow pattern close to the wall in electrochemical

0021-891X

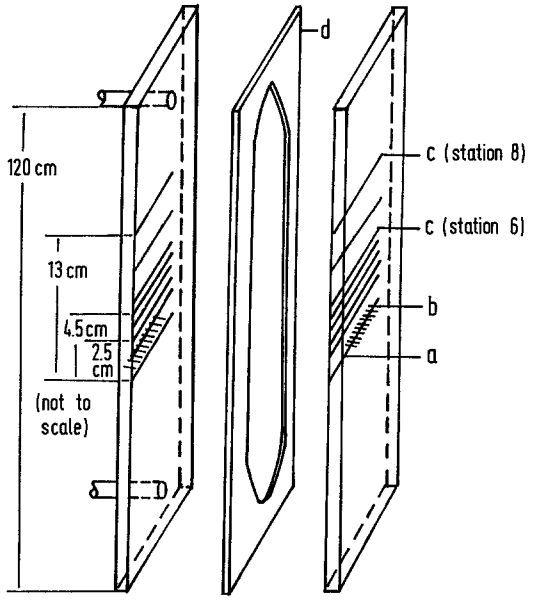

Fig. 1. Schematic of parallel flow electrochemical cell. (a) Copper marker, (b) platinum microelectrodes, (c) copper detectors and (d) spacer.

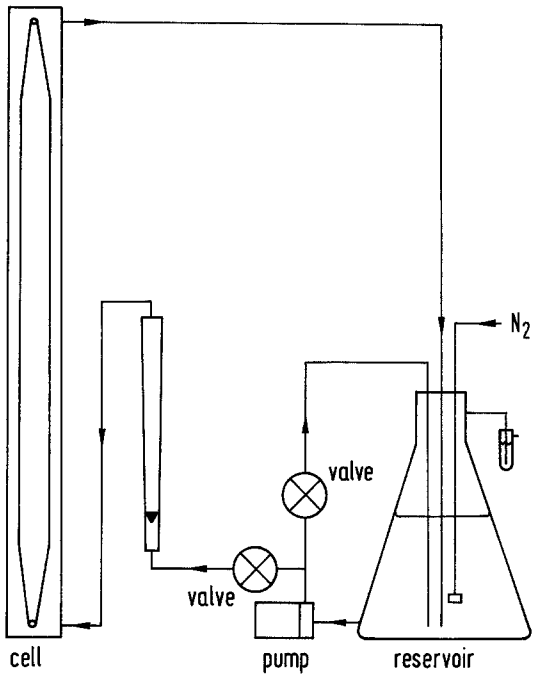

Fig. 2. Electrolyte flow system.

reactors has been previously studied [1,9–11]. These studies have employed stimulus–response techniques, with mostly an impulse signal as the stimulus [12]. This involves marking the stream of electrolyte with a concentration of copper ions equivalent to an impulse, by applying a short anodic pulse to the appropriate electrode. The response (concentration–time or C curve) measured at the detector electrode is the residence time distribution curve of the fluid under investigation. The C curve was modelled using the axially dispersed plug flow model [9,10], and the model parameters, namely, mean residence time (τ) and dispersion coefficient ($\bar{D}$) were obtained by time domain curve fitting.

This paper reports studies conducted to measure dispersion close to the wall in a parallel plate electrochemical reactor with electrodes flush-mounted on the walls, in the absence, as well as in the presence, of electrogenerated gas. Bubbles of hydrogen or oxygen gas were generated on platinum electrodes. Results on τ and $\bar{D}$, under a range of experimental conditions, are presented and discussed.

2. Experimental details

2.1. *Electrochemical cell design and flow system*

Figure 1 shows the electrochemical cell employed in this work. It consisted of three Perspex sheets, two outer slabs (1.0 cm thick) separated by a thin 0.2 cm thick spacer which defined the channel shape. The cell was sealed with a gasket of silicone rubber. Two pairs of aluminium angle beams running along the edge of the cell were through bolted to hold the cell together. A diffuser section (18 cm long, 8° half angle) was created before the parallel section to ensure fully developed flow in the cell for Reynolds' numbers up to 6000. The gap to width (i.e. aspect) ratio of the channel was 25, sufficient for the flow to be considered as one dimensional.

Copper electrodes (1.5 mm wide) were used as marker and detector electrodes, while platinum wires of 0.45 mm diameter were used to generate both oxygen and hydrogen bubbles. All these electrodes were flush-mounted on the walls in order to measure mixing close to the wall. Only the central portions of the copper detectors were in contact with the electrolyte, the edges being masked off with Lacomite to further reduce the effects of the side walls.

On each side of the cell, there were ten platinum microelectrodes equally spaced across the flow channel. These gas generating electrodes were individually controlled. This arrangement allowed the selection of bubble generation sites, bubble flow positions and dimension of bubble curtain. For all experiments with gas generation, constant current control was used. Selection of the polarity of the platinum electrodes gave oxygen or hydrogen as stirring gases.

A diagram of the fluid circuit is presented in Fig. 2 Electrolyte flow was induced by a small pump and was measured by a rotameter. The electrolyte was aqueous sulphuric acid (0.01 M) with copper sulphate (0.01 mM). Any oxygen in the electrolyte was removed by sparging with nitrogen gas.

2.2. *Measurement of dispersion*

An electrochemical analogue of the well known stimulus–response technique [12] for measuring dispersion, has been developed in Southampton [13,14]. An impulse or dirac delta signal was mainly employed as the stimulus. In these tests, the flow stream was marked with a Delta-function concentration pulse of copper ions by applying a short anodic pulse to a copper electrode (i.e. marker). The generated concentration pulse was equivalent to an impulse

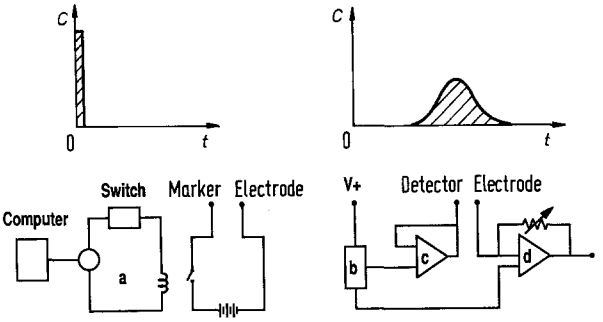

Fig. 3. Electric circuit for stimulus–response experiments. (a) Variable time circuit, (b) potentiometer, (c) voltage follower and (d) current follower.

stimulus. The response was measured at various distances downstream of flow using copper detector (electrodes, which were set at the potential of the diffusion limiting current so that the current drawn was a linear function of local copper ion concentration.

The pulsing circuit (Fig. 3) consisted of a bank of 9 V dry cell batteries connected in series with an electronically-timed reed switch. The length of pulses could be varied; 0.1 s was a typical width. The amplitude of the signal was 8.5 or 16.9 V. Voltage and current followers were used to buffer the potential of the detectors and to amplify the reduction current of copper deposition to a level sufficient for data acquisition by computer [11].

The response signal from the detector due to the impulse signal was acquired directly on to a computer and a data file was generated. Figure 4 shows a typical detector response curve for the wall phase. For measurements in the presence of bubbles, it was found necessary to acquire a few responses at each flow rate so that random noise could be averaged out. All experiments were conducted at room temperature (about 20° C).

Experimental response curves, after normalization, are modelled using the axially dispersed plug flow model [9,10,12]. This model assumes that there is no variation in composition in the radial direction, i.e. radial dispersion is negligible compared with axial dispersion. The two parameters in the model are:

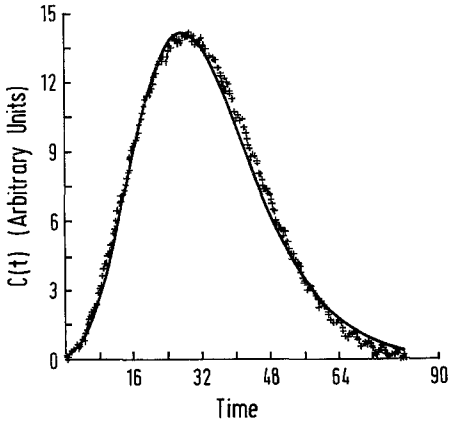

Fig. 4. Typical experimental response and fitting with dispersed plug flow model. (Re = 20, L = 2.5 cm, station 3). According to: (——) model and (+ + + +) experiment.

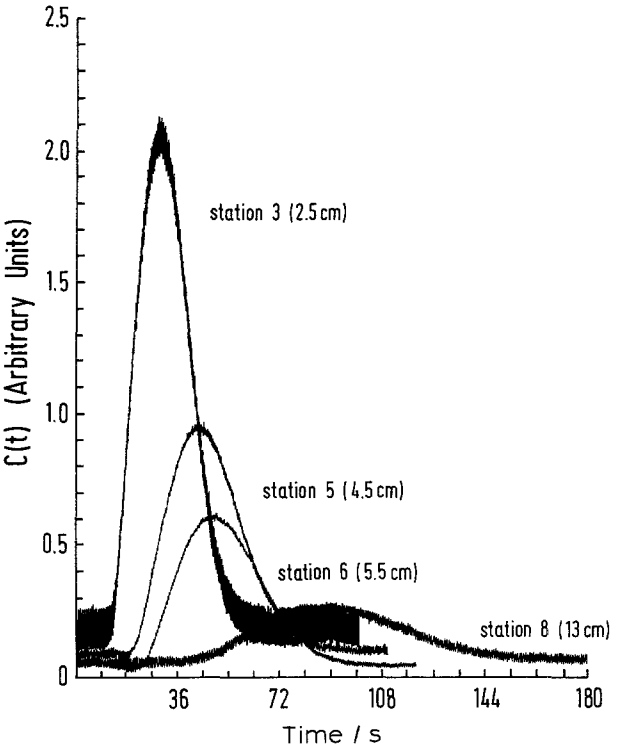

Fig. 5. Concentration–time curves at Re = 20.

mean residence time of the fluid, τ and Peclet number, Pe. The predicted (normalized) response according to this model is given by:

$$C(t) = \frac{Pe^{1/2}}{2\tau(\pi\theta)^{1/2}} \exp\left[-\frac{Pe(1-\theta)^2}{4\theta}\right] \quad (1)$$

where θ is the dimensionless time equal to t/τ. The Peclet number is defined as:

$$Pe = \bar{u}L/\bar{D} \quad (2)$$

where $\bar{u}$ is the average velocity of the fluid. Fluid in the bulk and close to the wall will have different average velocities. Since this study is concerned with flow and dispersion close to the reactor wall, $\bar{u}$ is taken as equal to L/τ, where L is the distance between marker and detector electrodes. Hence,

$$Pe = L^2/\bar{D}\tau \quad (3)$$

The parameters, τ and Pe in the model are evaluated by nonlinear least squares which involves matching the experimental response curve with that predicted by the model. Further details on this curve fitting are available in [15]. After obtaining Pe, $\bar{D}$ can be computed from Equation 3 since L is known.

3. Results and discussion

3.1. *Dispersion in the absence of gas*

Figure 5 shows typical responses to the impulse signal at various downstream detectors in the absence of gas bubbles. The effect of axial dispersion is to broaden the peaks as the distance from the marking electrode increases. Also, the area of the response curve generally decreases with distance, and this suggests some loss of copper ions from the wall phase to the rest of

Table 1. Ratio of mean residence time of marked material (τ) to that of bulk flow ($\bar{t}$) at various distances (L)

Re	*Ratio* ($\tau/\bar{t}$)		
	L = 2.5 cm	*L = 4.5 cm*	*L = 13.0 cm*
20	6.5	5.0	3.6
70	11.3	8.9	6.1
178	15.1	12.1	8.9
450	20.0	16.2	11.6

the fluid. All response curves, as illustrated in Fig. 4, can be well described by Equation 1. This indicates that the marked material, which remains in the vicinity of the wall (and hence fluid close to the wall), behaves as if it were in a regime of plug flow with axial dispersion.

The ratio of mean residence time of marked material (τ) to that of bulk flow ($\bar{t}$), is shown in Table 1. The mean residence time of marked material refers to that of fluid close to the wall only. As the flow rate (and hence Reynolds number) increases, the velocity gradient near the wall becomes steeper. This explains the increase of $\tau/\bar{t}$ with flow rate, and this increase is similar for all three L values. On the other hand, the ratio decreases with distance downstream because the marked material experiences some acceleration in its course by the faster core flow.

Results on mean residence time (τ) and dispersion coefficient ($\bar{D}$) are shown in Table 2. As expected, for a certain L, τ decreases as flow rate (or *Re*) increases, and Table 2 indicates that this decrease in τ with *Re* is comparable for the three distances studied. Data in Table 2 also show that τ increases with L at a given *Re*, but less than proportionally. This can be attributed to the acceleration of fluid close to the wall by the (relatively) fast moving core flow. Note that the thickness of the marked layer (y) is quite small. This can be calculated assuming that the fluid velocity near the wall ($\bar{u}$) is linearly related to the mean bulk velocity (U). This relationship is given by $\bar{u} = 6U(y/s)$, where s is the cell gap [16]. For the present experimental conditions, the thickness is in the range of 1–5% of cell gap. This is supported by the experimental finding that the marked material generated at the wall was not detected at either the midplane or the opposite wall.

Data on dispersion in the absence of gas (Table 2) show that $\bar{D}$ increases with flow rate (or *Re*) as well as with distance. However, the increase is less than proportionate, probably because the results are for flow close to the wall. However, increase in $\bar{D}$ with *Re* is similar for the three distances (L) studied. On the other hand, for a given *Re*, $\bar{D}$ increases with L more than proportionally. These results may be due to the effect of core flow on the fluid close to the wall, mentioned earlier.

Pe is plotted against *Re* (based on bulk flow) in Fig. 6. The small slope of the lines in Fig. 6 indicates that, as the bulk velocity (U) increases, the convective ($\bar{u}$) and dispersive ($\bar{D}$) forces on the marked material increase by approximately the same extent. Thus *Pe* is almost unaffected by *Re*.

3.2. *Dispersion in the presence of hydrogen gas*

Hydrogen gas was generated electrolytically at platinum microelectrodes, which were situated half-way between the marker and the first detector electrode (Fig. 1). Gas bubbles were small and spherical in shape, with a diameter in the range 50 to 200 μm [17]. Polarization curves for the copper deposition section at various detectors were first determined at different liquid and gas flow rates [11]. The potentials of the detector electrodes were then set to the voltage at the diffusion limiting current. Initially, system behaviour over a range of *Re* and gas generation conditions (e.g. number, position of microelectrodes as well as current to them), was observed.

One effect of the stirring caused by gas bubbles was a significant decrease in the signal to noise ratio. Consequently, only a limited range of measurements was possible; typical results are summarized in Table 2. In general, results for gas (either hydrogen or oxygen) evolution tend to have relatively large

Table 2. Mean residence time (τ) and dispersion coefficient ($\bar{D}$) in the absence and presence of electrogenerated hydrogen gas

L/cm	*Re*	*Mean residence time/s*			*Dispersion coefficient/cm s*$^{-2}$		
		τ_0	τ_{1Bb}	τ_{3B}	$\bar{D}_0$	$\bar{D}_{1Bb}$	$\bar{D}_{3B}$
2.5	20	29.8	28.4	23.6	0.0094	0.0103	0.0285
	70	15.5	15.3	15.0	0.0188	0.0212	0.0213
	178	8.2	7.9	8.0	0.0400	0.0402	0.0415
	450	4.6	4.7	4.6	0.0755	0.0787	0.0715
4.5	20	43.2	41.8	36.2	0.0193	0.0225	0.0415
	70	22.2	22.3	22.2	0.0391	0.0431	0.0413
	178	11.8	11.7	–	0.0789	0.0772	–
	450	6.7	6.8	6.6	0.1525	0.1505	0.1541
13.0	20	89.3	85.6	–	0.0715	0.1422	–
	70	43.9	43.9	–	0.1488	0.1988	–
	178	25.2	25.5	23.7	0.2888	0.2647	0.2877
	450	13.9	13.8	14.2	0.5587	0.5415	0.5222

Subscripts 0, 1, 3: number of microelectrodes used; B or Bb: low or high bubbling rate (9 or 20 mA/microelectrode).

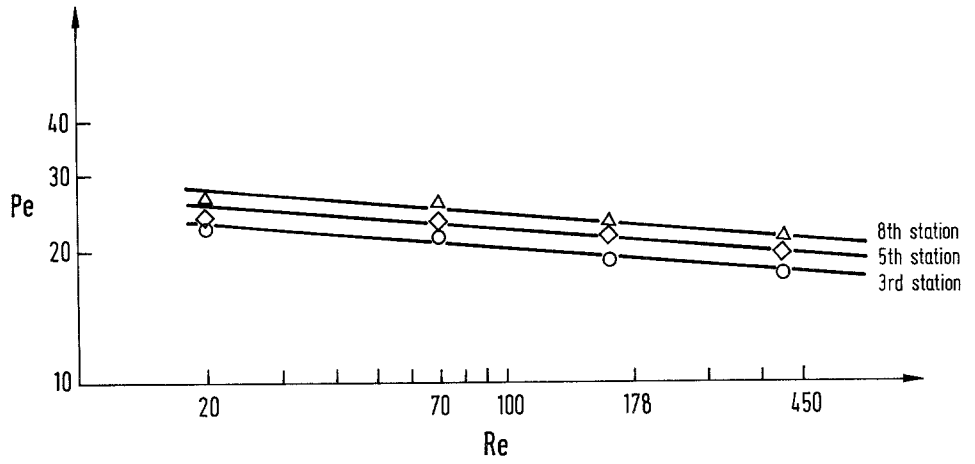

Fig. 6. Plot of Peclet number in the wall region against Reynolds number based on bulk velocity in the absence of gas bubbles.

experimental error and, consequently, scatter. This can be attributed to the macroscopic irreproducibility of the gas bubble - electrolyte flow. Note that the formation, travel and coalescence of gas bubbles are stochastic phenomena, and bubbles begin to adhere to the Perspex wall of the cell after a finite time. The latter phenomenon is a function of current, time and nature of the gas. Despite all these, the general trend is discernible.

The estimated mean residence time (τ) appears to be almost unaffected by gas stirring (Table 2). This could be because of small gas void fraction (less than 0.01) encountered in the present experiments. Dispersion ($\bar{D}$) is affected by hydrogen bubbles, mainly at low Re. The increase in $\bar{D}$ (Table 2) due to gas bubbling is particularly dramatic at $Re = 20$. Bubbles have almost no effect on $\bar{D}$ at higher Re (say, 170 and above).

The drastic increase of $\bar{D}$ at $Re = 20$ can be explained in terms of the bubble rise velocity in a swarm, u_b by [18]:

$$u_b = u_G + u_L + u_0 \tag{4}$$

where u_G and u_L are the superficial velocities of gas and liquid respectively, and u_0 is the rise velocity of a single bubble in a quiescent electrolyte. The last quantity can be predicted by the following equations [19]:

For $d \leqslant 100\,\mu m$

$$u_0 = \frac{d^2 g}{12\nu_L}\left(1 - \frac{\rho_G}{\rho_L}\right) \tag{5}$$

For $100 < d \leqslant 200\,\mu m$

$$u_0 = \frac{d^2 g}{36\nu_L} \tag{6}$$

Therefore, u_0 is 0.20 and 1.09 cm s^{-1} for $d = 50$ and 200 μm, respectively. At 3B bubbling rate (Table 2) and assuming 100% current efficiency:

$$u_G = \frac{\text{Total volumetric gas rate}}{\text{Reactor cross-sectional area}}$$
$$= 4.34 \times 10^{-3}\,\text{cm s}^{-1}$$

The liquid superficial velocity, u_L is 0.52 and 4.6 cm s^{-1} at $Re = 20$ and 178, respectively. So, u_G is negligible compared to other quantities in Equation 4.

Hence, at $Re = 20$, u_b is in the range 0.72 to 1.61 cm s^{-1} for bubble diameters 50–200 μm. Thus u_b is 40 to 200% more than the electrolyte velocity (u_L) depending on the bubble diameter. So it is plausible to suggest that turbulent eddies may well be caused by bubbles at low Re, leading to the increase in $\bar{D}$. On the other hand, the electrolyte velocity is much larger at higher Re. For example, u_L is 4.6 cm s^{-1} at $Re = 178$. Now, u_b is only 4 to 24% more than u_L. This implies that, at relatively high electrolyte velocity, the bubbles are carried away from their generation sites and may well be dispersed towards the faster moving core flow which, in effect, reduces the turbulence promoting effect of bubbles. Thus, at $Re = 178$ and 450 in Table 2, $\bar{D}$ and τ are almost unaffected by gas bubbles.

3.3. *Dispersion in the presence of oxygen gas*

In this study, six platinum microelectrodes were mainly used for gas generation. This arrangement provided a uniform curtain of gas flowing past the detector electrodes and led to more reproducible data. Different gas evolution rates (obtained by varying the gas current in the range 0 to 120 mA) at one liquid flow rate corresponding to $Re = 70$, were considered. Oxygen gas bubbles were observed to be spherical and generally bigger than the hydrogen bubbles.

For each gas current, void fraction (ε) can be calculated assuming 100% current efficiency and conversion to gas bubbles. The estimated ε is in the range 0 to 0.01 for the gas current range of 0 to 120 mA. It may be noted from [17,19,20] that practically all electrolytic gas generation has an ε value substantially smaller than unity, and the true value is very system dependent. Some parameters affecting ε, are pressure, temperature, current density, electrolyte flow rate and electrode material. The estimated ε reported here is likely to be much higher than in the reactor. Nonetheless, the void fraction within the reactor is small and well within the characterized bubble flow regime for two-phase flow. It may be noted that gas void fraction in industrial situations is generally much higher than 0.01.

Typical data on the effect of oxygen bubbles on τ and $\bar{D}$ at $Re = 70$ are presented in Table 3. For the

Table 3. Effect of oxygen gas on mean residence time (τ) and dispersion coefficient ($\bar{D}$) at Re = 70

τ/s or $\bar{D}$/cm s^{-2}	L/cm	Oxygen gas current				
		0 mA	10 mA	60 mA	90 mA	120 mA
τ	2.5	15.6	15.2	14.4	14.5	15.7
τ	4.5	22.6	22.0	20.9	21.0	21.9
τ	7.5	31.4	30.2	27.7	26.8	28.6
τ	13.0	43.9	43.5	–	35.9	36.1
$\bar{D}$	2.5	0.0190	0.0203	0.0206	0.0255	0.0233
$\bar{D}$	4.5	0.0370	0.0408	0.0508	0.0546	0.0594
$\bar{D}$	7.5	0.0644	0.0728	0.1132	0.0971	0.1592
$\bar{D}$	13.0	0.1107	0.1408	–	0.2345	0.3634

range of conditions studied, gas bubbles seem to have a negligible effect on τ when L is small. But τ appears to decrease marginally with increasing gas flow when L is large, say 7.5 or 13. This may be due to bubble coalescence during the travel over a longer distance resulting in larger bubbles, since the rise velocity of a single bubble is proportional to the square of bubble diameter (Equations 5 and 6). Hence, the velocity of bubbles is likely to increase significantly, affecting the adjacent liquid flow also.

Results in Table 3 show that $\bar{D}$ increases with gas current at a particular L. This increase is marginal when $L = 2.5$ and becomes significant as L takes larger values. A significant effect of oxygen bubbles on $\bar{D}$ at $L = 7.5$ or 13 is probably due to bubble coalescence and consequent increase in gas velocity. As with hydrogen bubbles, $\bar{D}$ increases with L more than proportionally at a particular gas current.

A few experiments at higher liquid flow rates (corresponding to $Re = 178$ and 450) were also conducted. These results are summarized in Table 4. Comparing the results in Tables 3 and 4, it can be concluded that $\bar{D}$ is almost unaffected by oxygen gas when the liquid flow rate is high.

3.4. *Comparison of mixing by hydrogen and oxygen bubbles*

This study was carried out at low gas rate (10 mA) and $Re = 70$. Six electrodes were employed, and the same side of the cell was used to improve reproducibility of hydrodynamic effects. Results for oxygen were taken from the previous section while experiments for hydrogen were conducted afresh in order to ensure identical experimental conditions. All these results are summarized in Table 5 for comparison purposes.

Table 4. Effect of oxygen gas on dispersion coefficient ($\bar{D}$) at higher liquid flow rates

Re	L/cm	Oxygen gas current		
		0 mA	50 mA	120 mA
178	2.5	0.041	0.041	0.044
178	4.5	0.079	0.079	0.078
178	5.5	0.129	0.135	0.139
450	2.5	0.076	0.076	0.075
450	4.5	0.153	0.157	0.163
450	5.5	0.229	0.249	0.275

Table 5. Comparison of mixing by hydrogen and oxygen bubbles at 10 mA gas current and Re = 70

L/cm	τ/s		$\bar{D}$/cm s^{-2}	
	Hydrogen	Oxygen	Hydrogen	Oxygen
2.5	15.5	15.2	0.0185	0.0203
4.5	22.4	22.0	0.0364	0.0408
7.5	30.6	30.2	0.0675	0.0728
13.0	43.0	43.5	0.1561	0.1408

It may be noted that hydrogen bubbles were generally smaller than oxygen bubbles, and that the total volume of hydrogen bubbles was roughly double that of oxygen bubbles (at the same gas current). Despite these differences, results in Table 5 indicate that τ is approximately the same for either hydrogen or oxygen gas. On the other hand, differences in $\bar{D}$ for hydrogen and that for oxygen, are less than 10%. Whether these differences are due to experimental error or different gas bubbles (size, number) is not clear.

4. Conclusions

The effect of electrogenerated hydrogen and oxygen bubbles on mixing or dispersion of marked material at the wall phase in a parallel plate electrochemical cell was studied. Experimental conditions were varied to cover Reynolds numbers up to 450, and (estimated) gas void fraction 0 to 0.01. The results obtained show that mean residence time (τ) of marked material is practically unaffected by gas evolution, and that the dispersion coefficient ($\bar{D}$) in the wall phase is a function of Reynolds number, distance (L) from the marker electrode and rate of gas production. $\bar{D}$ increases as gas evolution increases at low Reynolds numbers, say 20 or 70, and this increase becomes greater with distance from the marker electrode. On the other hand, at higher Re, say 170 and above, no significant change in dispersion is detected as compared to the dispersion in the absence of gas.

The described method of using platinum microelectrodes as gas generating agents has the advantage of forming bubbles of even size and having a good bubble distribution across the width of the cell. However it suffers from the problem of copper deposition at higher gas current leading to alteration of hydrodynamics within the cell, which is why experiments involving higher gas void fraction could not be carried out. Gas sparging through a porous membrane was also attempted, but the resultant bubbles had a non-uniform size distribution and were unevenly distributed across the flow channel.

References

[1] M. Fleischmann, J. Ghoroghchian and R. E. W. Jansson, *J. Appl. Electrochem.* **9** (1979) 437.
[2] C. W. Tobias, *J. Electrochem. Soc.* **106** (1959) 833.

[3] H. Vogt, *Electrochim. Acta* **26** (1981) 1311.
[4] B. Krause and H. Vogt, *J. Appl. Electrochem.* **15** (1985) 509.
[5] B. E. Bongenaar-Schlenter, L. J. J. Janssen, S. J. D. Van Stralen and E. Barendrecht, *ibid.* **15** (1985) 537.
[6] L. J. J. Janssen and E. Barendrecht, *Electrochim. Acta* **24** (1979) 693.
[7] K. Stephan and H. Vogt, *ibid.* **24** (1979) 11.
[8] H. F. M. Gijsbers and L. J. J. Janssen, *J. Appl. Electrochem.* **19** (1989) 637.
[9] R. E. W. Jansson and R. Marshall. *Electrochim. Acta* **27** (1982) 823.
[10] M. Fleischmann and R. E. W. Jansson, *J. Appl. Electrochem.* **9** (1979) 427.
[11] W. S. Wu, Ph.D. Thesis, Southampton University, Southampton, UK (1985).
[12] O. Levenspiel, 'Chemical Reaction Engineering', John Wiley, New York (1972).
[13] I. H. Justinijanovic, Ph.D. Thesis, Southampton University, Southampton, UK (1975).
[14] I. H. Justinijanovic and M. Fleischmann, *J. Appl. Electrochem.* **10** (1980) 143.
[15] G. P. Rangaiah and P. R. Krishnaswamy, *J. Chem. Eng., Japan* **23** (1990) 124.
[16] D. J. Pickett, 'Electrochemical Reactor Design', Elsevier, Barking, UK (1977).
[17] N. P. Brandon and G. M. Kelsall, *J. Appl. Electrochem.* **15** (1985) 475.
[18] L. Sigrist, O. Dossenbach and N. Ibl, *ibid.* **10** (1980) 223.
[19] H. Vogt, Gas Evolving Electrode, in 'Comprehensive Treatise of Electrochemistry', Vol 6 (edited by E. Yeager), Plenum Press, London (1983).
[20] H. Vogt, *J. Appl. Electrochem.* **17** (1987) 419.
[21] G. Kreysa and M. Kuhn, *ibid.* **15** (1985) 517.